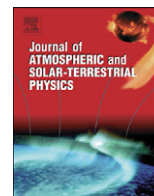




ELSEVIER

Contents lists available at SciVerse ScienceDirect

Journal of Atmospheric and Solar-Terrestrial Physics

journal homepage: www.elsevier.com/locate/jastp

Observation of a thermospheric descending layer of neutral K over Arecibo

Jonathan S. Friedman^{a,c,*}, Xinzhao Chu^b, Christiano Garnett Marques Brum^a, Xian Lu^b^a Arecibo Observatory, SRI International, HC-3 Box 53995, Arecibo, PR 00612, USA^b Cooperative Institute for Research in Environmental Sciences & Department of Aerospace Engineering Sciences, University of Colorado at Boulder, 216 UCB, Boulder, CO 80309, USA^c Puerto Rico Photonics Institute, Universidad Metropolitana, San Juan, PR 00926, USA

ARTICLE INFO

Article history:

Received 12 June 2012

Received in revised form

9 February 2013

Accepted 1 March 2013

Keywords:

Neutral K layer

Thermosphere

Descending ion layer

K Chemistry

Lidar

Arecibo

ABSTRACT

We report on the first observation of a descending layer of atomic potassium (K) in the thermosphere. This observation was made with the K Doppler lidar at the Arecibo Observatory in Puerto Rico (18.35°N; 66.75°W) on 12 March 2005. The layer was first observed before 08:00 UT (04:00 AST) centered near 145 km with the vertical extent up to ~155 km, and then it descended to near 126 km just over 2 h later at dawn. The descent rate of 2.56 ± 0.38 m/s matches the vertical phase speed of the GSWM09-computed semidiurnal tide between 120 and 150 km. This also matches the descent rates of the thermospheric semidiurnal tides measured at Arecibo. Although the K density above 120 km remains less than 1 cm^{-3} , its presence is unequivocal and has strong similarities to the neutral iron (Fe) layers in the thermosphere over 155 km recently discovered by lidar observations at McMurdo, Antarctica. The thermospheric K layer is plausibly explained by radiative electron recombination with K^+ within a tidal ion layer, which descends with the downward phase progression of the semidiurnal tide. Based on the production rate of K atoms and using current knowledge of tidal ion layer composition, we calculate an electron density of near $5 \times 10^4 \text{ cm}^{-3}$ and K^+ concentration of 650 cm^{-3} at 135 km immediately prior to the layer formation. This discovery of a thermospheric K layer, coupled with the McMurdo discovery of similar Fe layers, may lead to a new approach to studying the thermosphere in the altitude range of ~100–150 km with resonance fluorescence lidars.

© 2013 Elsevier Ltd. All rights reserved.

1. Introduction

Observations of neutral metal atoms have been reported in the lower thermosphere, up to 130 km as the ‘layer topside’ (Höffner and Friedman, 2004, 2005). These were first seen as the exponential decay of the topside of the main metal layer that is normally observed from roughly 80 to 105 km and attributed to micrometeoroid influx (Höffner and Friedman, 2004). In addition, specific events have been observed as high-altitude sporadic layers that occur up to 120 km, above and separate from the main layer (Collins et al., 1996; Gerding et al., 2001; Gong et al., 2003; Höffner and Friedman, 2005; Ma and Yi, 2010; Wang et al., 2012). These tend to exhibit downward phase propagation. From these observations, it appeared that neutral metal atoms did not exist above about 130 km. However, a recent report by Chu et al. (2011) has radically changed our view on the extension range of the neutral

metal atoms and hint at their source. Their report on the lidar observations of iron (Fe) over McMurdo, Antarctica, showed for the first time distinct, concentrated descending layers of neutral Fe atoms in the thermosphere, appearing at altitudes as high as 155 km with clear gravity wave signatures (Chu et al., 2011). Lübken et al. (2011), in work focused on temperature tides in the main Fe layer at Davis, Antarctica, reveal converged and descending Fe layers to 130–140 km, strongly supporting the McMurdo discovery. It is evident from the McMurdo layers that there is a relationship between ion layers enhanced in the descending phase front of a gravity wave or tide and the observed thermospheric neutral metal atom layers. Here, we report an event, similar to that observed over McMurdo, of a distinct layer of neutral potassium (K) atoms descending from ~150 km in the thermosphere over Arecibo.

The source of metal atoms and metallic ions in the thermosphere is not resolved. Höffner and Friedman (2004) speculate on a micrometeoroid source, and that the observed high altitude extensions were the result of direct meteor deposition of metal atoms. Sputtering of high-velocity, low mass meteoroids is possible in the 120–160 km altitude range, and in this mechanism

* Corresponding author at: Arecibo Observatory, HC03 Box 53995, Arecibo, PR 00612, USA.

E-mail address: jonathan@naic.edu (J.S. Friedman).

differential ablation is not a factor (Popova et al., 2007; Vondrak et al., 2008). However, neutral atoms released by meteoroid sputtering cannot directly account for narrow neutral layers in the thermosphere because of the high contrast and descent of the layers (Chu et al., 2011), although they may be a source for the metallic ions at high altitudes. At tropical latitudes meteoric metal ions are transported to the thermosphere by the equatorial fountain effect (Martyn, 1955; Duncan, 1960). This is expected to be limited to latitudes within about $\pm 20^\circ$ of the magnetic equator (Hanson and Moffett, 1966). However, Carter and Forbes (1999) have shown how this effect can contribute to the observed tidal ion layers (TILs) over Arecibo, whose geographic location at 18.35° N, 66.75° W is 28.5° N geomagnetic latitude.

Descending or tidal ion layers (TILs) are a ubiquitous feature of the thermosphere between 120 and 200 km over Arecibo (Bishop et al., 2000; Bishop and Earle, 2003; Mathews et al., 1993; Mathews and Morton, 1994; Earle et al., 2000). These are regularly observed with the incoherent scatter radar (ISR), but they have also been studied with in situ measurements using sounding rockets (Bishop et al., 2000; Roddy et al., 2007). They are thought to consist largely of metallic ions (Behnke and Vickrey, 1975; Tepley and Mathews, 1985; Bishop and Earle, 2003; Roddy et al., 2007). TILs are generated by compression of ionization in the E region by the descending phase front of a tide or gravity wave. They are formed through the electrodynamic coupling among the ions, the Earth's B -field, neutral wind shear, and local electric field (Mathews, 1998; Carter and Forbes, 1999).

During the pre-dawn hours of 12 March 2005, a neutral K layer was observed by the potassium resonance Doppler lidar in the thermosphere above the Arecibo Observatory. It first appeared around 08:00 UT (04:00 AST) centered at an altitude above 145 km and extending to near 155 km. The layer centroid descended to near 126 km at 10:14 UT, at which time observations were forced to end due to sunrise. Throughout the observations, the observable vertical extent of the layer was about 15 km. Until the observations of thermospheric Fe layers above McMurdo, we took this event to be a unique occurrence. The McMurdo events and the plausible explanations by Chu et al. (2011) have convinced us that the thermospheric K layer may not have been an anomaly, but may be correlated to a tidal ion layer rich in K^+ ions, which enhanced production of neutral K and made the layer detectable. The description of that event, discussion of its possible nature, and what this may portend for future studies of the thermosphere are the subject of this paper.

2. Observations

The K Doppler resonance lidar at Arecibo has been described in some detail (Friedman et al., 2003; Friedman and Chu, 2007). The 2005 observation of thermospheric K described here benefitted greatly from the optimizations required for best performance of a Doppler lidar, in that the signal is maximized through excellent transmitter performance and finely adjusted receiver throughput, and that background noise is minimized through finely tuned spatial and spectral filtering. This lidar is thus sensitive to very low metal densities (e.g., Höffner and Friedman, 2005), of under 0.1 cm^{-3} in 1.5 km bins and averaged over 12 min.

The observation discussed here is shown as the color contour plot in Fig. 1. The K densities are plotted logarithmically with 6-min integrations and 1-km range resolution, having been boxcar smoothed with a 12-min, 1.5-km window and rebinned from the original 1-min \times 0.15-km resolutions. Observations started shortly after midnight UT (20:00 AST), and the K layer morphology and behavior throughout most of the night appear to be fairly typical. A short-lived sporadic layer occurred around 103 km at about 01:00 UT

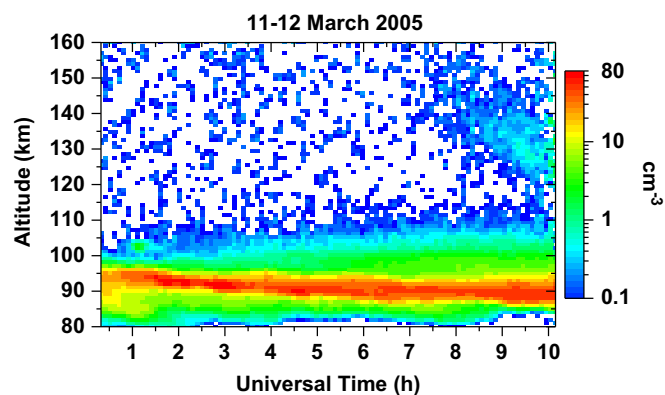


Fig. 1. A log-density range-time color plot of the potassium concentration above Arecibo on the night of 12 March 2005. The descending layer appearing above 145 km around 08:00 UT is the subject of this report.

and lasted for about 1 h. The upper extent of the main K layer at the beginning of observations was just over 100 km, and following the sporadic layer it climbed slowly, reaching over 110 km at dawn. The sharp lower edge began at slightly below 80 km and lifted to about 84 km, while being modulated by wave activity. At the same time, the main K layer peak presented an almost linear downward movement from ~ 95 km at $\sim 00:00$ UT to ~ 89 km at $\sim 10:00$ UT.

Separate from the main K layer, and beginning prior to 08:00 UT, a weak (peak $\sim 0.15 \text{ cm}^{-3}$) layer can be discerned centered near 145 km with a detectable vertical extent of over 10 km. The layer descends and strengthens over the subsequent two hours, until observations were forced to end due to sunrise (10:14 UT). At that point, the layer was centered at 126 km, with a ~ 20 km extent. The peak density of the layer increased during this time to near 0.75 cm^{-3} . To more clearly present the descending K layer, Fig. 2 shows the data isolated to the thermospheric layer. Panel (a) shows the data extracted from Fig. 1. For the contour in panel (b), we removed high-frequency noise by decomposing the signal in time and altitude and reconstructing the new signal (model) without the high frequencies (noise) using Finite Fourier series. This procedure was made possible by the fact that the measurements displayed dominant periodicities. For the thermospheric K density, its respective harmonics were calculated by altitude and each harmonic was leveled using the altitude as reference (for more details see Prado-Garzón et al., 2011). Panel (b) has a thick black line that tracks the thermosphere layer altitude center of mass, flanked by finer black lines showing the envelope within which the center of mass was calculated. In panel (c), we plot the center of mass altitude versus time along with a linear fit (red line). The fit shows the K layer descending at a near-constant rate of $9.20 \pm 1.36 \text{ km/h}$ ($2.56 \pm 0.38 \text{ m/s}$). Panel (d) of Fig. 2 shows the peak K concentration as a function of time, which increases throughout the measurement, as the layer descends.

In Fig. 3, we have plotted a single profile recorded in a 12-min integration around 09:08 UT (05:08 AST). This profile, plotted on a linear scale, shows the layer extent quite clearly from above ~ 120 to over 150 km, with a peak density of $\sim 0.55 \text{ cm}^{-3}$. Integrating through the individual profiles for data above 115 km (comfortably above the lower layer), we are able to show the contribution of this thermospheric K to the column abundance of K in Fig. 4. Up until almost 08:00 UT, there is no discernable K in the integrated data above 115 km, but after that time the K abundance rises rapidly, eventually reaching over 10^6 atoms in a 1 cm^2 cross-section column (values below 0 in Figs. 3 and 4 are the result of the statistical noise and mean background subtraction). The main K layer between 80 and 110 km at 09:08 UT exhibits a peak density and column abundance of 52.3 cm^{-3} and $3.1 \times 10^7 \text{ cm}^{-2}$, respectively.

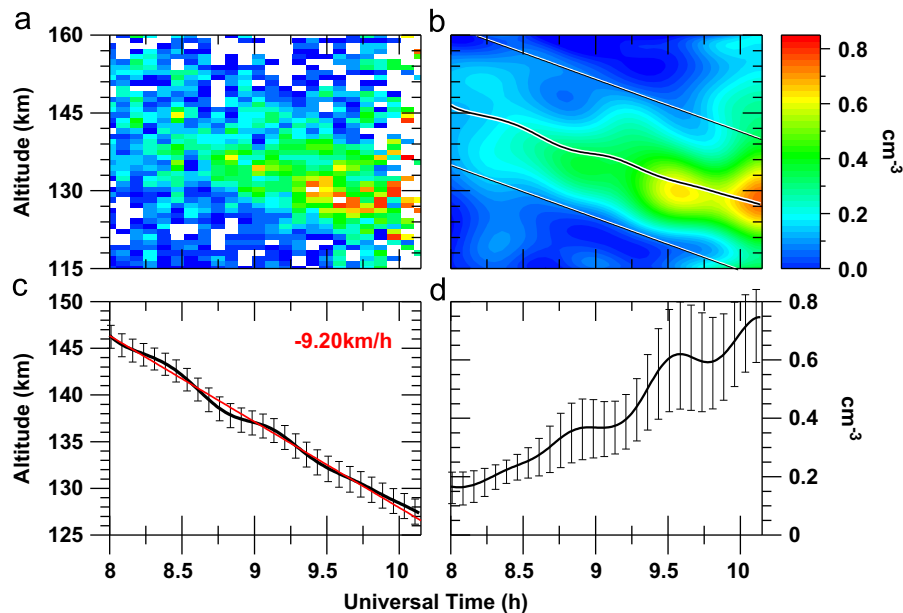


Fig. 2. (a) Lidar data showing the thermospheric K layer only; (b) Lidar data after removing high-frequency variation in both time and altitude, and including the layer center of mass (thick black line) as calculated between the thin gray lines; (c) Location of the layer center of mass in time and altitude plus a linear fit showing the descent rate and error bars indicating the RMS uncertainty, and; (d) Peak density of the layer as a function of time with statistical error bars.

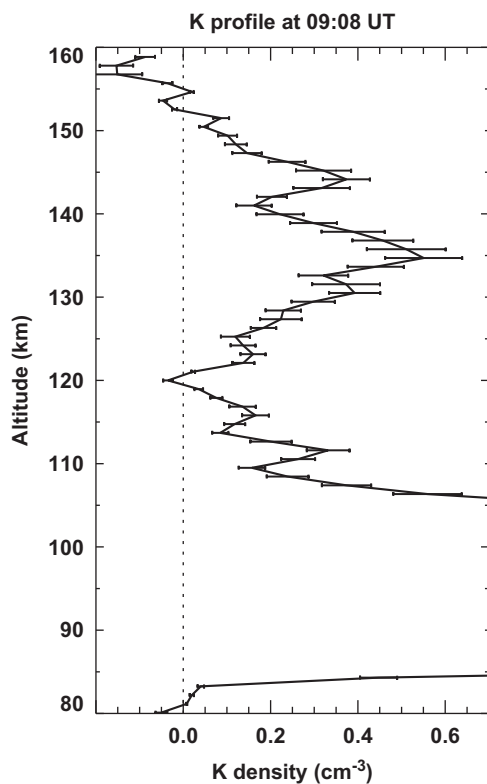


Fig. 3. A profile cut of the K layer over Arecibo at 09:08 UT (05:08) AST. Error bars show one standard deviation.

3. Discussion

3.1. Tidal Characteristics of the thermospheric K layer

The descending phase speed derived from the thermospheric K layer is measured to be 2.56 ± 0.38 m/s (Fig. 2c), which is slower than the descent rate of ~ 10 m/s observed in the thermospheric Fe

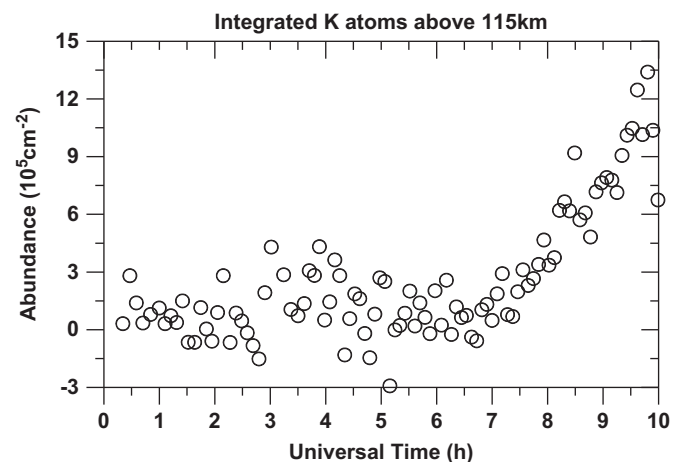


Fig. 4. Column abundance of K above 115 km altitude during the night of 12 March 2005.

layer at McMurdo, but it is consistent with the semidiurnal tide descent rate of ~ 2.5 m/s as calculated by the Global Scale Wave Model, GSWM09 (Zhang et al., 2010a,2010b). During the 1989 Arecibo Initiative in Dynamics of the Atmosphere (AIDA) campaign, from April 9–10, ion layers were observed descending from 150 to 120 km at a rate close to 2.5 m/s (Mathews et al., 1993). In a study of thermospheric tides over Arecibo, Zhou et al. (1997) report a vertical wavelength of 110 km at 144 km for the semidiurnal tide in zonal winds, implying a phase speed of 2.55 m/s, identical with the K layer discussed here. In this section we use GSWM09 to evaluate the possibility that the thermospheric K comes from K^+ in a TIL descending with the semidiurnal tide.

GSWM is a two-dimensional, linearized, steady state numerical tidal and planetary wave model that extends from the ground to the thermosphere (Hagan et al., 1995,1999). It solves the linearized perturbation equations in the presence of a background atmosphere, prescribed infrared and ultraviolet solar forcing, and dissipation profiles. Nonmigrating atmospheric tides are simulated in the earlier GSWM02 by including latent heat release associated

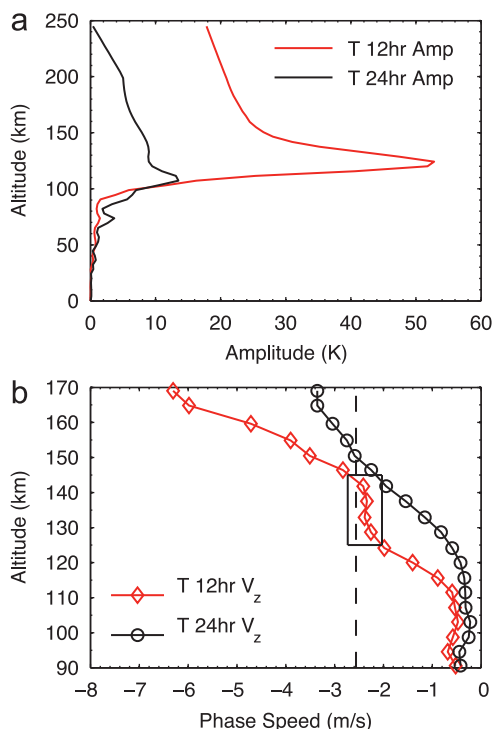


Fig. 5. GSWM09 computations of (a) amplitudes of diurnal (black) and semidiurnal (red) temperature tides, (b) same as (a) except for vertical phase speeds in m/s at Arecibo. The rectangle indicates the altitude range of the K observation.

with deep tropical convection (Hagan and Forbes, 2002,2003). New tidal solar radiative and latent heating rates based on the observations from the International Satellite Cloud Climatology Project (ISCCP) and Tropical Rainfall Measuring Mission were used for the GSWM09 update, and the results are shown to capture many observed features of tidal longitudinal variability (Zhang et al., 2010a,2010b). This is important for the interpretation of ground-based measurements. In this study, the semidiurnal tide retrieved from the GSWM09 includes both migrating and nonmigrating components, with wavenumbers from -6 to $+6$.

GSWM09 predicts that the amplitude of the semidiurnal thermal tide dominates over that of the diurnal tide in the thermosphere over Arecibo, as is shown in Fig. 5(a). Due to the longer vertical wavelength of the semidiurnal tide when compared to the diurnal tide, it is less susceptible to molecular viscosity in the altitude range of 120–150 km, and thus has larger amplitude in the thermosphere (Forbes, 1995). Fig. 5(b) shows the phase speeds of the GSWM09-computed diurnal and semidiurnal tides as a function of altitude (black and red lines, respectively). Most notable is the near-constant descent rate of ~ 2.5 m/s in the 130–150 km altitude range for the semidiurnal tide, which is denoted by the box surrounding the data. This is quite close to the 2.56 m/s descent rate of the observed neutral K layer (black vertical dashed line). The nearly constant phase speed of the semidiurnal tide would explain the nearly straight phase line of the observed K layer in this altitude range. In contrast, the vertical phase speed of the diurnal tide gradually varies with altitude, and it is normally 1–2 m/s, much smaller than that of the observed descending K layer. Given the large differences in phase speeds and amplitudes between 12-h and 24-h tides, if this observed K layer is indeed associated with tidal activity it is very likely that the semidiurnal tide, not the diurnal tide, is responsible for its downward progression.

The above tidal features predicted by GSWM09 are fully consistent with the results of Zhou et al. (1997) on the semidiurnal tides in the thermospheric zonal winds and temperatures over

Arecibo. Furthermore, Harper (1981) and Zhou et al. (1997) identify the semidiurnal tides as the strongest tidal component at Arecibo above 110 km, in good agreement with the GSWM09 results. The weight of past observations, the most modern and complete tidal modeling, and the characteristics of the observed thermospheric K layer together paint a convincing picture that, whatever the nature of the source and neutralization processes, the thermospheric K layer reported here is closely connected to the semidiurnal tide.

3.2. Formation of the thermospheric K layer

Descending thermospheric ion layers are tied to upward propagating tidal or gravity waves and descend with the phase progression of those waves. The waves produce compressed regions of ionization at the node where the winds above and below couple to the Earth's magnetic field and local electric field to force ions together, and the enhanced concentration of ions and electrons makes them detectable with instruments such as ISRs. These layers are known to produce very high metal ion concentrations (Chimonas and Axford, 1968; Mathews and Bekeny, 1979; Bishop and Earle, 2003), and if those concentrations are sufficient, radiative recombination should occur at high enough levels to make lidar-detectable neutral metal atom concentrations as argued in Chu et al. (2011). Unlike the ions, the neutrals are not electrodynamically tied to the wind node of the descending gravity wave phase front, so there is no a priori reason to believe that we are observing the same K atoms as the layer descends. Rather, the continuing descent of the layer indicates production of new K atoms, so recombination must continue as long as the neutral metals are detectable. Because of the similar phase speed as discussed above and considerable supporting evidence from prior observations (e.g., Harper, 1981; Mathews et al., 1993; Zhou et al., 1997), we hypothesize that the observed thermospheric K layer is linked to a descending TIL rich in K^+ ions. However, neither the tide nor a TIL alone is sufficient to explain the observation of the thermospheric K layer as these are ubiquitous and common features of the thermosphere above Arecibo, but the layer is apparently a rare event at Arecibo. Thus, it is the purpose of this section to determine conditions of a TIL that could result in the observed K layer.

In our analysis below, we consider only ion-neutral chemistry leading to net production of neutral K locally, neglecting horizontal advection due to the one-dimensional nature of the observations. We base this analysis assuming the existence of a thermospheric TIL, in which the ion concentration, or at very least K^+ ion concentration, reaches a level where neutralization exceeds ionization, and a detectable level of K atoms results. The observation of neutral K in a descending layer above 130 km is taken to be the result of production in a TIL through radiative electron recombination, which is shown in Reaction R1. In order for this mechanism to function, the production rate of neutral K must exceed the ionization rate via charge transfer causing loss of K. Reaction R2 shows the formula for charge transfer.



Formulating the net production rate results in Eq. (1):

$$R = k_{K^+} [K^+] [e^-] - (k_{O_2} [K] [O_2^+] + k_{NO^+} [K] [NO^+]) \quad (1)$$

where R is the net production rate, k_{K^+} is the radiative recombination rate coefficient, $[K^+]$ is the concentration of K^+ ions, $[e^-]$ (also denoted as N_e) is the concentration of electrons, $k_{O_2^+}$ and k_{NO^+} are the charge transfer ionization rate coefficients for $M = O_2^+$

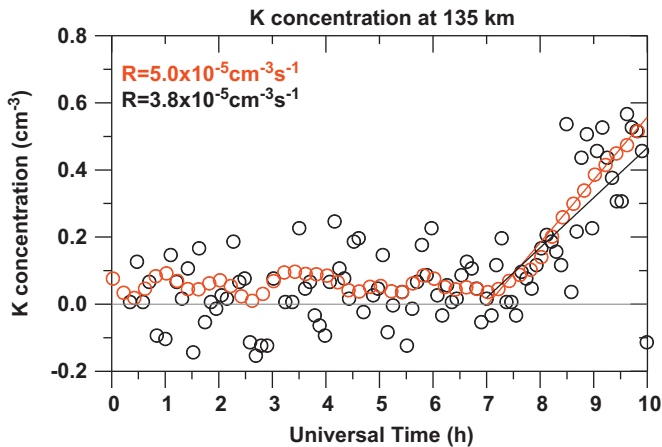


Fig. 6. K concentration at 135 km altitude during the night of 12 March 2005. Black and red circles represent the data and the reconstruction of [K] without the high frequencies, respectively, along with their linear fits.

and NO^+ , respectively, and [K], $[\text{O}_2^+]$ and $[\text{NO}^+]$ are the concentrations of each of these components of the reactions.

We evaluate the layer at an altitude of 135 km, which is indicative of the production and where the signal-to-noise ratio is relatively high. Figs. 1 and 2 indicate that at 135 km the initiation and peak of the layer are both observed before sunrise. These are required for the subsequent analysis. In Fig. 6, we show the production of K at 135 km in both the original and filtered data (black and red circles, respectively). The filtered data allow us to determine a starting time for production of K. Fitting a line to the filtered data after that time gives an estimate for the production rate for that altitude, in this case $R \approx 5 \times 10^{-5} \text{ cm}^{-3} \text{ s}^{-1}$. Recombination by Reaction R1 is very slow, with a rate coefficient of (Plane et al., 2006; Pavlov, 2012)

$$k_{\text{K}^+} = 2.63 \times 10^{-12} (300/\text{Te})^{0.9} \text{ cm}^3/\text{s} \quad (2)$$

Meanwhile, the rate coefficients for the molecular ions in Reaction R2 are measured to be $k_{\text{O}_2^+} = 5.6 \times 10^{-9} \text{ cm}^3/\text{s}$ and $k_{\text{NO}^+} = 4 \times 10^{-9} \text{ cm}^3/\text{s}$ (Delgado et al., 2006), as reflected in Eq. (1). The substantially higher rates for charge transfer ionization both put stringent requirements on the availability of K^+ ions and support the assumption of localized neutralization.

At the time when production of neutral K begins, charge exchange ionization of neutral K cannot occur because there are no K atoms, so the second term on the right hand side of Eq. (1) is zero, and the measured production rate is simply $R = k_{\text{K}^+} [\text{K}^+] [e^-] = 5 \times 10^{-5} \text{ cm}^{-3} \text{ s}^{-1}$ with no loss term. Next, assuming that the neutralization has negligible impact on the overall ionization, we presume that this term is conserved during the layer lifetime. Once neutral K atoms are produced, the second (depletion) term of the right hand side of Eq. (1) kicks in. This leads to the equilibrium state over two hours later, when the layer peaks so $R=0$, and the depletion term is also equal to $5 \times 10^{-5} \text{ cm}^{-3}/\text{s}$.

At this point, we employ the rocket-borne mass spectrometer results of Roddy et al. (2007) to provide the molecular fractions. They find that the fraction of O_2^+ is nearly negligible ($\ll 1\%$) at the altitudes of interest. This allows us to say, from the right hand side of Eq. (1), that $k_{\text{NO}^+} [\text{K}] [\text{NO}^+] = 5 \times 10^{-5} \text{ cm}^{-3}/\text{s}$. At $R=0$, [K] is $\sim 0.5 \text{ cm}^{-3}$, which leads to the result that $[\text{NO}^+] = 2.5 \times 10^4 \text{ cm}^{-3}$. This value is high, considering the current reference model (IRI) ambient value of ca. $\sim 600 \text{ cm}^{-3}$ for Arecibo's location at this date and time (Bilitza, 2001). However, Arecibo TILs have often been observed with concentrations greater than 10^4 cm^{-3} (Earle et al., 2000; Roddy et al., 2007).

Roddy et al. (2007) also found that molecular ions correspond to roughly half of the ionization in the observed intermediate layers.

Taking that assumption, we then determine that $[e^-] \sim 5 \times 10^4 \text{ cm}^{-3}$. Applying this to the initial case, when $t=0$, and employing NRLMSISE-00 (Picone et al., 2002) to give us a value for electron temperature T_e of 544 K, we find that $[\text{K}^+] = 650 \text{ cm}^{-3}$. Thus, K^+ constitutes $\sim 1.3\%$ of the total ionization (2.6% of the total metals). We have so far found only one report of K^+ abundance in the thermosphere from rocket-borne mass spectrometer measurements, which gives its concentration to be 0.33% of the measured metal ions (including Fe^+ , Na^+ , Mg^+ , Al^+ , K^+ , Ca^+ , and Ni^+), though these measurements represent an integration from 70 to 115 km (Kopp, 1997). Therefore, the K^+ ratio estimated above is about one order of magnitude larger than the result of Kopp (1997). This is also the case when comparing to the neutral metal concentration ratios between 110 and 125 km reported by Höffner and Friedman (2004,2005). On the other hand, our estimate is compatible with the results of Delgado et al. (2012), who show that a sporadic E layer centered near 103 km above Arecibo contained 1.55% K^+ .

It is worth pointing out that the above results are based on the assumption that the K production is solely achieved through (direct) radiative electron recombination with K^+ ions. If it is possible for dissociative electron recombination to operate, then the K^+ concentration required could be much less than that derived above. However, dissociative recombination is not anticipated for altitudes over 120 km, based on studies of Fe and K layers (Plane, 2003; Zhou et al., 2008; Chu et al., 2011; Delgado et al., 2012). Thus, we feel that radiative recombination is the only effective neutralization process above 120 km, which in turn demands high K^+ concentration. This requires convergence of available ions in a layer, and a source of extra K^+ . Given the 1-dimensional nature of the observations, we do not know if dynamical or electrodynamic effects may have converged background ionization horizontally. It is conceivable that horizontal convergence could compress hundreds of km of ions down to tens of km, thus concentrating K^+ to the required levels, though this would in turn produce a much higher overall level of ionization. Detailed investigation of such a mechanism is beyond the scope of this paper and should be addressed in future collaborative modeling and observational efforts.

Finally, we investigated other possibilities of correlative data that could indicate a source of the thermospheric K. Carter and Forbes (1999) predicted that under highly-active circumstances the equatorial fountain effect could reach Arecibo's latitude. This would deposit metal ions from equatorial regions to higher latitudes, and potentially seed the observed layer. Total electron content (TEC) measurements reveal the fountain effect by detecting the geographic distribution and dynamics of TEC. However, investigation of TEC data for this period (not shown here) found no activity to indicate an active fountain effect.

4. Conclusions

We have reported on a March 2005 observation of a thermospheric layer of neutral potassium atoms descending from an altitude centered near 145 km, with upper extent reaching 155 km, to about 126 km. Although the K density above 120 km is less than 1 cm^{-3} , its presence is unequivocal and has strong similarities to the lidar observations of thermospheric Fe layers at McMurdo, Antarctica (Chu et al., 2011). This is, to our knowledge, the first observation of such a phenomenon of a K layer in the thermosphere above 130 km. In contrast to the multiple phase fronts of the descending thermospheric Fe layers observed at McMurdo, the downward phase progression of the K layer was observed only once because Arecibo observations were ended by sunrise. While the McMurdo Fe layers exhibit a clear gravity wave downward phase progression, the Arecibo K layer morphology is

similar to that of the GSWM09-computed semidiurnal thermal tide, as both have descending rates near the measured 2.5 m/s. Furthermore, the observed K layer shape and phase speed are also very similar to prior observations of semidiurnal tides and tidal ion layers at Arecibo. This leads us to hypothesize that the descending thermospheric K layer is possibly the result of neutralization of K^+ ions within a tidal ion layer that descends with the downward phase progression of the semidiurnal tide. With this hypothesis, we have computed the ion density at 135 km, assuming radiative electron recombination as the neutralization process and charge transfer from NO^+ to K as the ionization loss process. By considering only ion-neutral chemistry leading to net production of neutral K locally while neglecting horizontal advection due to the one-dimensional nature of the observations, our estimate requires a moderately strong TIL with peak ion densities exceeding $5 \times 10^4 \text{ cm}^{-3}$ and a K^+ ion concentration of 650 cm^{-3} at 135 km.

Combining these characteristics with the thermospheric K layer morphology and descent rate, we find it convincing that the observed neutral K is the product of neutralization of K^+ ions within a TIL carried downward by the semidiurnal tide. However, TILs are common over Arecibo, while this neutral layer is a rare event. In over 150 nights and 1000 h of K lidar observations at Arecibo, we have only one such detection of a descending thermospheric K layer above 130 km. This implies that this particular TIL was unusual, and its unusual characteristic is in the K^+ concentration. The calculated K^+ concentration (650 cm^{-3}) corresponds to 1.3% of the total ions (2.6% of the metals), which is about an order of magnitude higher than other measurements of metal ions in the thermosphere. Because K layers are observed occasionally as high as 130 km at Arecibo, there is likely a metal ion reservoir that acts as a source for these layers. As it is known that Fe^+ and Mg^+ dominate the converged ion layers in the E region, thermospheric layers consisting of neutral Fe should be far more observable than those consisting of K. This is borne out in the Antarctic observations (Chu et al., 2011; Lübken et al., 2011). Furthermore, near-ideal observing conditions are required to detect the low signals when atom densities fall under $1/\text{cm}^3$, and such conditions are present for only a fraction of the ~ 1000 h of total data. This will certainly impact the detection frequency of thermospheric metal layers. Nevertheless, as noted above we have found a number of K layers that reach above 120 km, even as high as 130 km at Arecibo. Therefore, neutral metal atom layers in the thermosphere probably occur more frequently than they are observed, and it is probable that if observed in Fe (or even Na), they will be seen with higher frequency.

These results point to a potential opportunity for the resonance lidar community. There is a great desire to extend the altitude range of lidar detection to 100–200 km. We hope this may be partly addressed through the discovery of metal atoms in the thermosphere. Resonance lidars for the detection of meteoric metals have greatly matured and are broadly distributed throughout the world. In particular, the development of resonance fluorescence Doppler and Boltzmann lidar technologies have enabled the probing of winds and temperatures. Considerable progress has been made in improving system efficiencies, which are now getting close to theoretical optimum. Should these improvements result in more detections of neutral metal atom layers above 110 km, we see this as potentially a new method to study the thermosphere, measuring neutral temperatures and winds along with metal atom densities by resonance fluorescence lidar.

Acknowledgments

We gratefully acknowledge the contribution from Xiaoli Zhang, who provided GSWM-09 tidal data and insightful discussion. We

also acknowledge the contribution of Néstor Aponte for providing TEC data. We appreciate valuable discussions with Jia Yue, Qihou Zhou, and Rebecca Bishop. We are grateful to two anonymous reviewers, whose feedback led us to substantially improve the manuscript. The Arecibo Observatory is operated by SRI International, in a consortium with Universidad Metropolitana and Universities Space Research Association, under a cooperative agreement with the National Science Foundation. JF and XC acknowledge support from NSF grant ATM-0535457. XC acknowledges support from NSF grants ANT-0839091 and AGS-1136272. The Cooperative Institute for Research in Environmental Sciences (CIRES) is a joint institution of the National Oceanic and Atmospheric Administration and the University of Colorado. XL is grateful for support provided by the CIRES postdoctoral visiting fellowship.

References

- Behnke, R.A., Vickrey, J.F., 1975. Radar evidence for Fe in a sporadic-E layer. *Radio Science* 10 (3), 325–327.
- Billitz, D., 2001. International reference ionosphere 2000. *Radio Science* 36 (2), 261–275, <http://dx.doi.org/10.1029/2000RS002432>.
- Bishop, R.L., Earle, G.D., Herrero, F.A., Bateman, T.T., 2000. Observations of an intermediate layer during the Coqui II campaign. *Journal of Geophysical Research* 105 (A11), 24963–24971, <http://dx.doi.org/10.1029/1999JA000453>.
- Bishop, R.L., Earle, G.D., 2003. Metallic ion transport associated with mid-latitude intermediate layer development. *Journal of Geophysical Research* 108 (A1), 1019, <http://dx.doi.org/10.1029/2002JA009411>.
- Carter, L.N., Forbes, J.M., 1999. Global transport and localized layering of metallic ions in the upper atmosphere. *Annales Geophysicae* 17, 190–209.
- Chimonas, G., Axford, W.I., 1968. Vertical movement of temperate-zone sporadic E layers. *Journal of Geophysical Research* 73 (1), 111–117.
- Chu, X., Yu, Z., Gardner, C.S., Chen, C., Fong, W., 2011. Lidar observations of neutral Fe layers and fast gravity waves in the thermosphere (110–155 km) at McMurdo (77.8°S, 166.7°E), Antarctica. *Geophysical Research Letters* 38, L23807, <http://dx.doi.org/10.1029/2011GL050016>.
- Collins, R.L., Hallinan, T.J., Smith, R.W., Hernandez, G., 1996. Lidar observations of a large high-latitude sporadic Na layer during active aurora. *Geophysical Research Letters* 23, 3655–3658.
- Delgado, R., Weiner, B.R., Friedman, J.S., 2006. Chemical model for mid-summer lidar observations of mesospheric potassium over the Arecibo Observatory. *Geophysical Research Letters* 33, L02801, <http://dx.doi.org/10.1029/2005-GL024326>.
- Delgado, R., Friedman, J.S., Fentzke, J.T., Raizada, S., Tepley, C.A., 2012. Sporadic metal atom and ion layers and their connection to chemistry and thermal structure in the mesopause region at Arecibo. *Journal of Atmospheric and Terrestrial Physics* 74, 11–23, <http://dx.doi.org/10.1016/j.jastp.2011.09.004>.
- Duncan, R.A., 1960. The equatorial F region of the ionosphere. *Journal of Atmospheric and Terrestrial Physics* 20, 167–176.
- Earle, G.D., Bishop, R.L., Collins, S.C., González, S.A., Sulzer, M.P., 2000. Descending layer variability over Arecibo. *Journal of Geophysical Research* 105 (A11), 24951–24961, <http://dx.doi.org/10.1029/2000JA000029>.
- Forbes, J.M., 1995. Tidal and planetary waves. In: Johnson, R.M., Killeen, T.L. (Eds.), *The Upper Mesosphere and Lower Thermosphere: A Review of Experiment and Theory*. Geophys. Monogr. Ser., vol. 87. American Geophysical Union, pp. 67–87.
- Friedman, J.S., Tepley, C.A., Raizada, S., Zhou, Q.H., Hedin, J., Delgado, R., 2003. Potassium doppler-resonance lidar for the study of the mesosphere and lower thermosphere at the Arecibo Observatory. *Journal of Atmospheric and Terrestrial Physics* 65 (16–18), 1411–1424, [http://dx.doi.org/10.1016/S1364-6826\(03\)00205-0](http://dx.doi.org/10.1016/S1364-6826(03)00205-0).
- Friedman, J.S., Chu, X., 2007. Nocturnal temperature structure in the mesopause region over the Arecibo Observatory (18.35°N, 66.75°W): Seasonal variations. *Journal of Geophysical Research* 112, D14107, <http://dx.doi.org/10.1029/2006JD008220>.
- Gerding, M., Alpers, M., von Zahn, U., 2001. Sporadic Ca and Ca^+ layers at mid-latitudes: Simultaneous observations and implications for their formation. *Annales Geophysicae* 19, 47–58.
- Gong, S.S., Yang, G.T., Wang, J.M., Cheng, X.W., Li, F.Q., Wan, W.X., 2003. A double sodium layer event observed over Wuhan, China by lidar. *Geophysical Research Letters* 30 (5), 1209, doi: 2002GL016135.
- Hagan, M.E., Forbes, J.M., Vial, F., 1995. On modeling migrating solar tides. *Geophysical Research Letters* 22 (8), 893–896.
- Hagan, M.E., Burrage, M.D., Forbes, J.M., Hackney, J., Randel, W.J., Zhang, X., 1999. GSWM 98: Results for migrating solar tides. *Journal of Geophysical Research* 104 (A4), 6813–6827, <http://dx.doi.org/10.1029/1998JA900125>.
- Hagan, M.E., Forbes, J.M., 2002. Migrating and nonmigrating tides in the middle and upper atmosphere excited by tropospheric latent heat release. *Journal of Geophysical Research* 107 (D24), 4754, <http://dx.doi.org/10.1029/2001JD001236>.

- Hagan, M.E., Forbes, J.M., 2003. Migrating and nonmigrating semidiurnal tides in the upper atmosphere excited by tropospheric latent heat release. *Journal of Geophysical Research* 108 (A2), 1062, <http://dx.doi.org/10.1029/2002JA009466>.
- Hanson, W.B., Moffett, R.J., 1966. Ionization transport effects in the equatorial F region. *Journal of Geophysical Research* 71 (23), 5559–5572.
- Harper, R.M., 1981. Some results on mean tidal structure and day-to-day variability over Arecibo. *Journal of Atmospheric and Terrestrial Physics* 43 (3), 255–262, [http://dx.doi.org/10.1016/0021-9169\(81\)90047-7](http://dx.doi.org/10.1016/0021-9169(81)90047-7).
- Höffner, J., Friedman, J.S., 2004. The mesospheric metal layer topside: a possible connection to meteoroids. *Atmospheric Chemistry and Physics* 4, 801–808.
- Höffner, J., Friedman, J.S., 2005. The mesospheric metal layer top side: examples of simultaneous metal observations. *Journal of Atmospheric and Terrestrial Physics* 67, 1226–1237, <http://dx.doi.org/10.1016/j.jastp.2005.06.010>.
- Kopp, E., 1997. On the abundance of metal ions in the lower ionosphere. *Journal of Geophysical Research* 102 (A5), 9667–9674, <http://dx.doi.org/10.1029/97JA00384>.
- Lübken, F.-J., Höffner, J., Viehl, T.P., Kaifler, B., Morris, R.J., 2011. First measurements of thermal tides in the summer mesopause region at Antarctic latitudes. *Geophysical Research Letters* 38 (L24), 806, <http://dx.doi.org/10.1029/2011GL050045>.
- Ma, Z., Yi, F., 2010. High-altitude sporadic metal atom layers observed with Na and Fe lidars at 30°N. *Journal of Atmospheric and Terrestrial Physics* 72 (5-6), 482–491, <http://dx.doi.org/10.1016/j.jastp.2010.01.005>.
- Martyn, D.F., 1955. Theory of height and ionization density changes at the maximum of a Chapman-like region, taking account of ion production, decay, diffusion, and total drift, *Proceedings Cambridge Conference*, 255–259, Physical Society, London.
- Mathews, J.D., Bekeby, F.S., 1979. Upper atmosphere tides and the vertical motion of ionospheric sporadic layers at Arecibo. *Journal of Geophysical Research* 84, 2743–2750.
- Mathews, J.D., Morton, Y.T., Zhou, Q., 1993. Observations of ion layer motions during the AIDA campaign. *Journal of Atmospheric and Terrestrial Physics* 55 (3), 447–457.
- Mathews, J.D., Morton, Y.T., 1994. Radar measurements of dynamics and layering processes in the 80–150 km region at Arecibo. *Advances in Space Research* 14 (9), 153–160.
- Mathews, J.D., 1998. Sporadic E: current views and recent progress. *Journal of Atmospheric and Terrestrial Physics* 60, 413–435.
- Pavlov, A.V., 2012. Ion chemistry of the Ionosphere at E- and F-region altitudes: a review. *Surveys in Geophysics* 33 (1), 1–40, <http://dx.doi.org/10.1007/s10712-012-9189-8>.
- Picone, J.M., Hedin, A.E., Drob, D.P., Aikin, A.C., 2002. NRLMSISE-00 empirical model of the atmosphere: statistical comparisons and scientific issues. *Journal of Geophysical Research* 107 (A12), 1468, <http://dx.doi.org/10.1029/2002JA009430>.
- Plane, J.M.C., 2003. Atmospheric chemistry of meteoric metals. *Chemical Reviews* 103, 4963–4984.
- Plane, J.M.C., Plowright, R.J., Wright, T.G.J.A., 2006. Theoretical study of the ion-molecule chemistry of $K^+ \cdot X$ complexes ($X=O, O_2, N_2, CO_2, H_2O$): implications for the upper atmosphere. *Journal of Physical Chemistry A* 110 (9), 3093–3100, <http://dx.doi.org/10.1021/jp054416g>.
- Popova, O.P., Strelkov, A.S., Sidneva, S.N., 2007. Sputtering of fast meteoroids' surface. *Advances in Space Research* 39, 567–573, <http://dx.doi.org/10.1016/j.asr.2006.05.008>.
- Prado-Garzón, D., Brum, C., Echer, E., Aponte, N., Sulzer, M.P., González, S.A., Kerr, R. B., Waldrop, L.S., 2011. Response of the topside ionosphere over Arecibo to a moderate geomagnetic storm. *Journal of Atmospheric and Terrestrial Physics* 73 (11), 1568–1574, <http://dx.doi.org/10.1016/j.jastp.2011.02.016>.
- Roddy, P.A., Earle, G.D., Swenson, C.M., Carlson, C.G., Bullett, T.W., 2007. The composition and horizontal homogeneity of E region plasma layers. *Journal of Geophysical Research* 112, A06312, <http://dx.doi.org/10.1029/2006JA011713>.
- Tepley, C.A., Mathews, J.D., 1985. An incoherent scatter radar measurement of the average ion mass and temperature of a nighttime sporadic layer. *Journal of Geophysical Research* 90, 3517–3519.
- Vondrak, T., Plane, J.M.C., Broadley, S., Janches, D., 2008. A chemical model of meteoric ablation. *Atmospheric Chemistry and Physics* 8, 7015–7031.
- Wang, J., Yang, Y., Cheng, X., Yang, G., Song, S., Gong, S., 2012. Double sodium layers observation over Beijing, China. *Geophysical Research Letters* 39 (L15801), <http://dx.doi.org/10.1029/2012GL052134>.
- Zhang, X., Forbes, J.M., Hagan, M.E., 2010a. Longitudinal variation of tides in the MLT region: 1. Tides driven by tropospheric net relative heating. *Journal of Geophysical Research* 115, <http://dx.doi.org/10.1029/2009JA014897>.
- Zhang, X., Forbes, J.M., Hagan, M.E., 2010b. Longitudinal variation of tides in the MLT region: 2. Relative effects of solar radiative and latent heating. *Journal of Geophysical Research* 115, <http://dx.doi.org/10.1029/2009JA014898>.
- Zhou, Q.H., Sulzer, M.P., Tepley, C.A., 1997. An analysis of tidal and planetary waves in the neutral winds and temperature observed at low-latitude E region heights. *Journal of Geophysical Research* 102 (A6), 11,491–11,505, <http://dx.doi.org/10.1029/97JA00440>.
- Zhou, Q., Raizada, S., Tepley, C.A., Plane, J.M.C., 2008. Seasonal and diurnal variation of electron and iron concentrations at the meteor heights above Arecibo. *Journal of Atmospheric and Terrestrial Physics* 70, 49–60, <http://dx.doi.org/10.1016/j.jastp.2007.09.012>.